The impact of vessel size, orientation and intravascular contribution on the neurovascular fingerprint of BOLD bSSFP fMRI

Mario Gilberto Báez-Yánez [1,2], Philbert S. Tsai[3], David Kleinfeld[3,4] and Klaus Scheffler[1,5*]

[1] Department of High-Field Magnetic Resonance, Max Planck Institute for Biological Cybernetics, Tuebingen, Germany.
[2] Graduate Training Centre of Neuroscience, University of Tuebingen, Tuebingen, Germany.
[3] Department of Physics, University of California at San Diego, La Jolla, CA, USA.
[4] Section of Neurobiology, University of California, La Jolla, CA, USA.
[5] Department of Biomedical Magnetic Resonance, University of Tuebingen, Tuebingen, Germany.
* mario.baez@tuebingen.mpg.de

Zusammenfassung: Basierend auf Monte Carlo Simulationen wurden oxygenierungs-abhängige Signaländerungen bei balanced SSFP, Gradienten- und Spinechosequenzen untersucht. Signaländerungen wurden für künstliche Zylinder und reale neurovaskuläre Netzwerke aus dem Kortex der Maus mit 1 μm Auflösung berechnet. Signaländerungen als Funktion des Gefäßdurchmessers, dem Blutvolumen, der Gefäßorientierung zum Magnetfeld sowie das Verhältnis der intra- und extravaskularen Beiträge wurden berechnet. Die Resultate zeigen, dass bSSFP eine hohe Sensitivität sowohl für intra- als auch extravaskuläre Komponenten zeigt. Außerdem zeigen Gradientenechos und bSSFP, aber weniger SE, eine starke Signaländerung mit der Orientierung der Gefäße zum äußeren Magnetfeld.

Motivation

Modelling the functional nuclear magnetic resonance signal opens the possibility to go beyond the actual magnetic resonance imaging resolution and to extract the fingerprint of mesoscopic structure immersed in an image voxel.

Analytical and numerical calculations based on artificial vascular networks are the most used methods to model the physiological implications that a neural activation and its related hemodynamics processes in a functional magnetic resonance imaging experiment influence the NMR signal behavior.

Infinitely long cylinders mimicking the neurovascular structure is a well-known model to infer NMR signal behavior changes for specific parameters [5], such as radius size, orientation to the main magnetic field, susceptibility difference with the medium; but still a more realistic model is needed to disentangle the basis of the functional signal.

The ability to resolve cortical layers and columns depends ultimately on the scale; laminar and columnar fMRI can only be visualized if the cortical vasculature is imaged at scales beyond the penetrating arterioles, i.e., at the level of the capillary bed [2], and if the used fMRI sequence is sensitive to that level.

Imaging at 7T or 9.4T therefore opens the possibility to resolve structures far below the thickness of 2-3 mm of the human neurocortex. Anatomical images with an isotropic resolution below 200 μm have been obtained at 9.4T [8] that clearly resolve subcortical structures. Therefore, at very high fields the BOLD response from single cortical layers or other mesoscopic substructures might be resolved.

If an fMRI method is more sensitive to capillaries than to arteries/veins, the method is said to be more specific, since the location of the functional activation is presumably closer to the location of the neural activity. Spatial specificity of blood oxygenation level dependent (BOLD) contrast NMR signals at intracortical level could benefit from the precise quantitative evaluation of the vascular network and suggested approximations by numerical simulation and analytical solutions [3].

An open question is the origin of signal formation in bSSFP, which is of crucial importance to interpret the quality of BOLD bSSFP data with respect to the underlying neurovascular function.

This paper focuses on the analysis and description of the neurovascular fingerprint of pass-band bSSFP, an imaging modality that has been introduced for functional BOLD imaging in 2001 (at the stop-band [7]), and that was further advanced by several groups [9,12].

The formation of NMR signal from water proton magnetization during a random walk through the neurovascular network was modeled using Monte Carlo simulations for artificial cylinders with different diameter and orientation, as well

as for four different sets of neurovascular networks (Fig.1) acquired from the mouse parietal cortex measured with two-photon laser scanning microscopy at 1 µm isotropic resolution [4]. In addition, selected Monte Carlo simulations of GE and SE have been performed to serve as a comparison to pass band bSSFP.

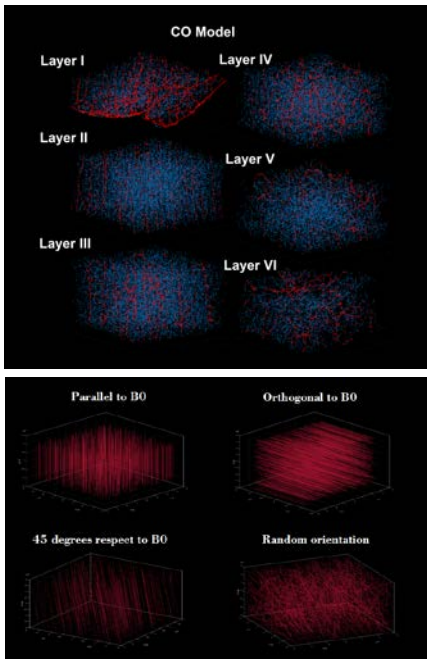

Fig. 1: Depiction of the neurovascular model divided in 6 equidistant layers. The macrovessels are in red, while the capillary bed (microvessels) are in blue. This data was acquired with two-photon laser imaging technique [4]. Moreover, random position cylinder model in different orientation respect B0.

Material and Methods

We analyze four vasculature network datasets from mice parietal cortex acquired with two-photon laser imaging technique [4] and the effect that a well organize vascular structure produce in the NMR signal under a BOLD contrast experiment (de-/oxygenated state), as well as for random positioned cylinders.

Gradient Echo (GE), Spin Echo (SE) and pass-band balanced Steady-State Free-Precession (bSSFP) sequences were simulated. For GE and SE, we follow the same procedure as Weisskof and Boxerman [1, 5] to obtain the NMR signal decay. To calculate the behavior of the bSSFP spin magnetization, 3x3 matrix Bloch equation were solved. Spin diffusion motion was simulated with random walkers [6]. Susceptibility inhomogeneities were calculated based on oxygenation level and orientation respect B0 [5].

Results

We first consider a comparison of the sensitivity to the vessel radius between GE, SE and pass-band bSSFP (Fig.2). These simulations are based on cylinders at random orientation occupying different BV fractions from 1%to 5%. In accordance with past results [1, 5], GE has an unspecific sensitivity to all vessel sizes larger than about 5 µm as a consequence of static dephasing, and a linear dependence of the signal change with BV (Fig.2a). Similarly, SE shows its typical selectivity to vessel radii between 2 to 10 µm and almost no signal change for larger vessels in the static refocusing regime (Fig.2b). As for GE, the peak sensitivity in SE scales linearly with the fractional BV. The bSSFP profile is similar to the SE profile (Fig.2b,c), however, it does not return to zero sensitivity for larger vessels, and has a slightly broader response to the vessel size in accordance to previous work [6].

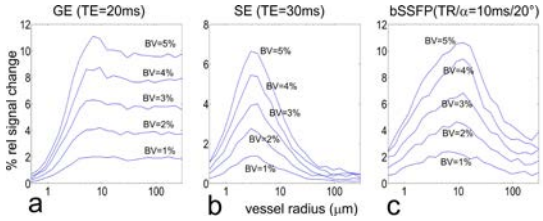

Fig. 2: BOLD signal change of GE, SE and bSSFP as a function of vessel radius (randomly oriented cylinders) for different fractional BV. Blood oxygenation of Y=77% and Y=85% was assumed for the resting and activated state, respectively, at a field strength of 9.4T.

The dependence of the BOLD bSSFP signal change as a function of different TRs and flip angle is shown in Fig.3. All simulations show a peak around small vessel radii of about 2 to 10 µm which slightly varies with the chosen TR. With increasing TR (Fig.3a-c) the vessel size selectivity shifts to larger radii and the peak signal change is strongly increased, i.e., by a factor of 3-4 going from TR=5ms to 20ms. Also, for longer TR, greater than approximately 10ms, the contribution from larger vessels (> 100 µm) increases to up to 50% of the peak signal. The BOLD-related signal change increases with flip angle up to about 20° by a factor of about 2-3, and shows no further increase for higher flip angles (Fig.3d-f).

In Fig.4, only parallel cylinders with a certain angle to B0 have been simulated. This mimics a very simplified model of parallel diving (penetrating) veins and arteries oriented perpendicular to the cortical surface. For GE, basically all vessel radii exhibit a strong dependence of the signal change on the cylinder orientation to B0. For bSSFP simulated at TR = 5 ms, only small vessels (1 to 10 µm) depend on their angle to B0, larger vessels just give a very small signal change, which is similar to the SE behavior shown right. As the bSSFP sensitivity to larger vessels

increases with TR (see Fig.3), the bSSFP simulation using TR = 15 ms shows some signal dependence on orientation to B0 also for larger vessels around 50 to 200 µm.

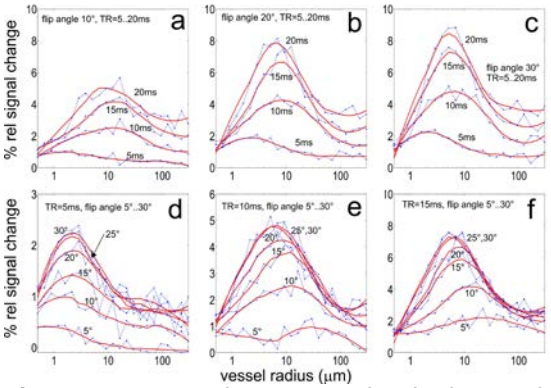

Fig. 3: Extravascular BOLD signal change for bSSFP for different TR and flip angles as a function of the vessel radius (red lines are polynomial fits to the simulation results (in blue)). Blood oxygenation of Y=77% and Y=85% was assumed for the resting and activated state, respectively, at a field strength of 9.4T. Intravascular blood T2 was set to T2=12ms for the resting state and T2=20ms for the activated state. The fractional BV of the randomly oriented cylinders was set to 2% for all simulations.

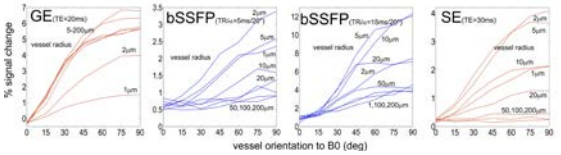

Fig. 4: BOLD signal change as a function of the orientation of the vessel (cylinder) to B0 for GE, bSSFP and SE for different vessel radii ranging from 1 to 200 µm, and for a fractional BV of 2%.

Simulations based on reconstructed cortical neurovascular network were performed by dividing each network into six equally spaced layers starting from the top showing the large cortical surface vessels (layer 1) down to the boundary of grey and white matter (layer 6) (right panels, Fig.6A-D). The Larmor frequency distribution within the layers was calculated by the Finite Perturber Method. As layer 1 includes the large cortical surface vessels, the corresponding frequency distribution is much broader compared to deeper layers (left panels, Fig.5A-D). However, the layer-specific frequency distributions show a large variation across the four different data sets.

The signal changes shown in the right part of Fig.5 are strongest for the surface layer 1, and they decrease by about a factor of 4 to 6 for GE and about 2 to 3 for SE and bSSFP going towards the deeper layers. The simulated functional signal change for GE (TE=20ms), SE (TE=30ms) and bSSFP (TR/α=5ms/20°), as well as local fractional BV for each layer, is seen (right panels, Fig.5A-D). Functional signal changes were calculated for two orientations of the vessel network to B0, 0° (dotted line, surface perpendicular to B0) and 90° (solid line, surface parallel to B0). For GE, a very strong signal change increase can be observed towards the surface layer 1 which is less pronounced for bSSFP and SE. A certain dependence on the orientation to B0 is visible for all modalities, but is strongest for GE. The effect on orientation is inverted, starting from the surface layer to deeper layers, and occurs since surface vessels are mostly perpendicular to the penetrating vessels.

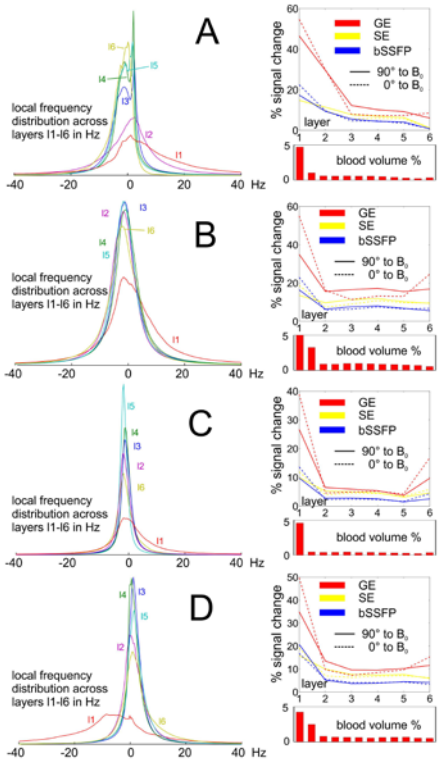

Fig. 5: The left column shows the frequency distribution (assuming $\Delta\chi$ = 0.22x10-7 at 9.4T and with the top surface of the vessel network oriented perpendicular to B0) around the vessel network for layers l1 to l6 for the four different data sets A to D shown in Fig. 6. The right column shows BOLD signal changes for GE (TE=20ms), SE (TE=30ms) and bSSFP (TR/α=5ms/20°) across layers l1 to l6 oriented perpendicular (0°, dotted line) and parallel (90°, solid line) to B0 and their respective blood volume fraction.

The signal change dependence on the orientation of the cortex to B0 is summarized in Fig.6.The left column shows renderings of the four vectorized vessel data sets of the mice parietal cortex. The three columns on the right show signal changes for GE (TE=20ms), SE (TE=30ms) and bSSFP (TR/α=5ms/20°) as a function of the orientation to B0, where for 0° and 180° the penetrating vessels are parallel, and surface vessels are perpendicular to B0. The calculated signal changes are relative to the change observed at 90° and were calculated in percent by 100 x ($\Delta S_{\theta z}$-

$\Delta S_{90°})/\Delta S_{90°}$ for each of the six layers and for the mean signal across layers shown in red.

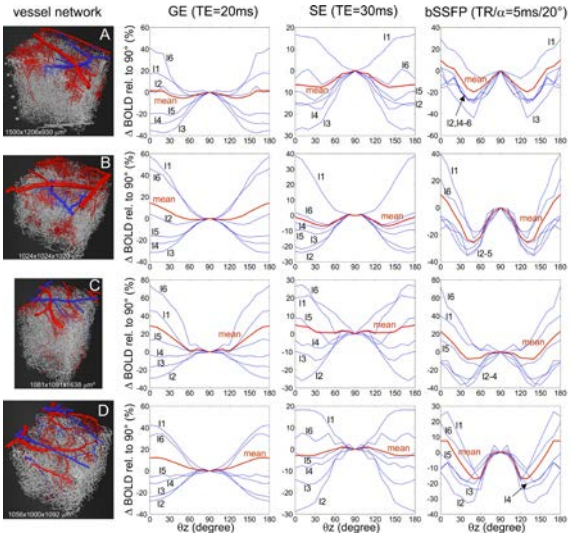

Fig. 6: The left column depicts the rendered vessel data sets used for Monte Carlo simulations. The three right columns show the orientational and layer-specific dependence of GE, SE and bSSFP as relative percentage change to the reference at 90° (layer surface parallel to B0 or penetrating vessels perpendicular to B0). The red curves are the mean through all layers, i.e. represent the BOLD response of the entire cortical structure. For simplicity, orientations for $\theta > 90°$ were set equal to those of $\theta_{>90°} = 180° - \theta_{<90°}$.

Discussion

The presented results are all based on Monte Carlo simulations assuming a certain global oxygenation change between Y = 77% and Y = 85%, and for a field strength of 9.4T. In general, the frequency pattern around cylinders or vessels scales linearly with oxygenation and field strength, and thus the resulting signal change strongly depends on these parameters. However, the basic characteristics of the presented plots, such as the selectivity to a certain vessel radius, the dependence on the fractional BV and the orientational dependence, do not depend on the particular choice of the selected parameters. Similar shapes of signal changes as a function of the vessel size and fractional BV have been reported for GE, SE and bSSFP [1,5,6]. Similarly, the choice of relaxation times of the extra- and intravascular space have an impact on the overall signal changes, and more significantly also on the relation of intra- and extravascular contributions.

- **Specificity to the capillary and non-capillary network**

The well-known behavior of GE, SE and pass-band bSSFP as a function of vessel (cylinder) size could be confirmed in Fig.2. Experimental comparisons between GE and bSSFP in functional checker board experiments at 9.4T, however, show a lower signal change for bSSFP compared to GE [12], in contrast to signal changes presented in Fig. 2. This might be related to the vessel size selectivity of bSSFP, as larger vessels contribute to GE but less to bSSFP. Compared to SE, bSSFP shows a slightly larger contribution for vessels larger than 50 µm, which can be attributed to the stronger intravascular effect compared to SE.

The shape as well as the peak of the curve that describes the bSSFP signal change as a function of vessel radius depend on TR and flip angle. The curves shown in Fig. 3 are similar to those shown in other publications that used largely different parameters for their simulations [6]. An increase in TR gives a much higher signal change, and in parallel, an increasingly contribution from larger vessels (> 50 µm). An increase of the flip angle to about 20° to 25° also boosts the signal change as shown in the bottom row of Fig. 3. The contribution of vessels larger than 50 µm is less pronounced for increasing flip angles (bottom row in Fig. 3) than for increasing TRs (top row). For experimental applications a longer TR of 10 to 15 ms thus seems to be beneficial. In addition, higher flip angles can be used due to the lower power deposition. A drawback of longer TRs at very high fields is increased banding artifacts.

According to the plots in Fig. 2 and 3, the BOLD signal ratio, which can be defined as the ratio of the contributions from the laminar vasculature and from intracortical veins, is significantly different for GE, SE and bSSFP. The BOLD signal ratio, i.e. the selectivity to oxygenation changes in capillaries and venules is highest for SE, followed by bSSFP (depending on TR of bSSFP) and is much lower for GE. However, it should be noted that most functional studies using SE are based on SE-EPI readouts that show a T2* decay around the spin echo that is usually placed in the center of k-space. The resulting T2*-related blurring will thus introduce a certain GE-type weighting, depending on the resolution and acceleration factor. Thus, as bSSFP only acquires one single k-space line per TR, the GE contribution in bSSFP might be comparable or even less compared to SE-EPI.

Furthermore, all sequence show an increased BOLD signal change towards the cortical surface, as shown in Fig. 5. The frequency distribution around the vessels based on the measured optical data set depends on the layer level. The observed signal change thus depends on the chosen resolution of the functional imaging sequence: if a single voxel covers the entire thickness of the cortex, about

50% of the signal change is produced by surface vessels for GE, but only about 10 to 20% for SE and bSSFP (assuming an isotropic resolution of 2-3 mm as commonly used in functional studies). Thus, SE and bSSFP capture significantly more responses from deeper layers compared to GE. At higher resolution, however, the BOLD signal ratio becomes more similar across sequences, except for the surface layer 1.

- **Orientational bias**

The dependence of the signal change on the orientation of the cortex to B0 clearly demonstrates, that the vessel structure is highly oriented and far from being a randomly oriented set of cylinders. Furthermore, there seems to be a striking difference of the orientational signal dependence in bSSFP compared to GE and SE: while the angular signal dependence in GE and SE mostly shows one period of signal changes within 0° to 180°, the bSSFP response for single layers as well as for the mean across layers seems to be slightly bi-periodic. This is also partially the case for SE but only for the mean response. However, it remains open if this bi-periodic behavior can be generalized to different cortical areas or even to humans, or subcortical vessel networks. A similar, mono-periodic dependence has been reported by [10] based both on experiments and Monte Carlo simulations. However, these data show a much stronger angular dependence for GE compared to SE (bSSFP was not analyzed there). The dependence of the signal change on the orientation of the cortex to B0 has implications for any quantitative or calibrated measurement of oxygenation changes or contrast agent-induced susceptibility changes as used, for example, in first-pass contrast-enhanced perfusion measurements. The derived results of such studies might be strongly biased by the local orientation of the cortex to B0.

- Limitations of this study

In general, a limitation of this study is the simplified assumption of a certain susceptibility difference between all vessels types and surrounding tissues without any dynamic and spatially varying patterns of oxygenation and blood volume changes. Therefore, our results do not contribute to the question, whether layer-specific neuronal activation can be detected with GE, SE or bSSFP. However, disentangling responses from different layers probably requires a detailed knowledge of the spatially resolved oxygenation and blood volume dynamics. Furthermore, the BOLD signal characteristics of GE, SE and bSSFP are related to the vessel architecture of the mouse parietal cortex. An analysis of other cortical or subcortical regions in animals or humans would be of high interest, however, to our knowledge currently no such high-resolution data is available. Another critical parameter is diffusion of water across the vessel boundary at high fields. The very short T2 or T2* of blood together with diffusion into and out of the vessels act as a relaxation mechanism. In our simulation we assumed non-permeable vessels**.**

Summary

For future reference of the complete publication, see [11]

References

1. Weisskoff RM et al. Microscopic susceptibility variation and transverse relaxation: theory and experiment. Magn Reson Med (1994) 31:601-610
2. Goense J et al. fMRI at high spatial resolution: implications for BOLD models. Front Comput Neurosci (2016) 10:66
3. Lauwers F et al. Morphometry of the human cerebral cortex microcirculation: general characteristics and space related profiles. NeuroImage (2008) 39:936-948
4. Blinder P et al, The cortical angiome: an interconnected vascular network with noncolumnar patterns of blood flow. Nature Neurosci (2013) 16:889-897
5. Boxerman J et al. MR contrast due to intravascular magnetic susceptibility perturbations. Magn Reson Med (1995) 34:555-566
6. Bieri O Scheffler K. Effect of diffusion in inhomogeneous magnetic fields on balanced steady state free precession. NMR Biomed (2007) 20:1-10
7. Scheffler, K., et al., 2001. Detection of BOLD changes by means of frequency-sensitive TrueFISP technique: preliminary results. NMR Biomed. 14, 1-7.
8. Budde, J., et al., 2014. Ultra-high resolution imaging of the human brain using acquisition-weighted imaging at 9.4T. Neuroimage. 1 (86), 592-8.
9. Miller, K.L., 2102. FMRI using balanced steady-state free precession (SSFP). NeuroImage 62, 713–719
10. Gagnon, L., et al., 2015. Quantifying the microvascular origin of BOLD-fMRI from first principles with two-photon microscopy and an oxygen-sensitive nanoprobe. J. Neurosci. 35 (8), 3663–3675.
11. Baez-Yanez M.G. et al, The impact of vessel size, orientation and intravascular contribution on the neurovascular fingerprint of BOLD bSSFP fMRI, NeuroImage (2017) doi: 10.1016/j.neuroimage.2017.09.015.
12. Scheffler, K., Ehses, P., 2015. High-resolution mapping of neuronal activation with balanced SSFP at 9.4 tesla, Magn. Reson. Med. 76, 163-171.